Expansion dynamics of Lennard-Jones systems

M. J. Ison,[1,2,*] F. Gulminelli,[2] and C. O. Dorso[1]
[1]*Departamento de Física, Facultad de Ciencias Exactas y Naturales, Universidad de Buenos Aires, Buenos Aires (1428), Argentina*
[2]*LPC Caen, ENSICAEN, Université de Caen, CNRS/IN2P3, Caen, France*
(Received 4 October 2007; published 10 March 2008)

The dynamics of the expansion of a Lennard-Jones system, initially confined at high density and subsequently expanding freely in a vacuum, is compared with an expanding statistical ensemble derived in the diluted quasi-ideal Boltzmann approximation. The description proves to be fairly accurate at predicting average one-body global observables, but important deviations are observed in the configuration-space structure of the events. Possible implications for finite expanding physical systems are outlined.

DOI: 10.1103/PhysRevE.77.031109 PACS number(s): 64.10.+h, 25.75.Ld, 05.10.−a

I. INTRODUCTION

When a finite isolated unbound system decays in a vacuum, its decay pattern is often characterized by an ordered kinetic component: the collective flow. This is the case in cluster dissociation induced by photoionization [1–4] or charge transfer collisions [5,6]. Here, the condensed matter bulk limit encourages, in principle, an interpretation in terms of liquid-vapor transition. However, the obvious fact that all vapor flows out and no vapor comes back in makes it difficult to push the analogy further and the dynamical evaporation can only be interpreted thermodynamically [1,2,5] by making use of a time-dependent temperature within the concept of an evaporative ensemble [7,8]. Flow is also a basic feature of heavy ion collisions, where the products of fragmentation reactions show a velocity preferentially oriented in the radial direction [9]. If in the low-energy regime and in the associated multifragmentation phase transition these collective flows are only a perturbation in the global energetics, this is not true at higher energies (between 0.2 and 2.0 GeV/nucleon), where they are likely to influence light cluster formation by coalescence [10]. In the ultrarelativistic regime, the ordered and disordered motions become comparable in magnitude [18] and collective flows are believed to play an essential role in the characteristics of the transition to the quark-gluon plasma observed in the Relativistic Heavy Ion Collider data [11–13].

In the initial stage of a nuclear collision, the complexity of the dynamics is such that a statistical analysis of the system might prove useful, even at low energies. If this equilibrium stage occurs at high density [14], the final-state interaction may still be important in the subsequent evolution and it is not clear how the final partitions at the freeze-out stage, where the fragment interactions are assumed to have ceased, will be modified. In a previous paper [15] we addressed this issue at the classical level through molecular dynamics simulations of a Lennard-Jones system [16], initially thermalized at high (supercritical) density and subsequently expanding freely in the vacuum. We have shown that the dynamics of the expansion leads to a considerable increase of fluctuations. By the time the partitions are settled and the formed prefragments cease to interact (freeze-out), these fluctuations are qualitatively similar to the ones expected for a thermal system at reduced subcritical density. A naturally arising question is then whether the expanded system at freeze-out can still be treated as a statistical equilibrium at a lower density.

This important question, which probably does not have a unique answer, can only be addressed by our numerical experiments in a very partial and incomplete way. In the evaporation regime accessed in cluster experiments, a freeze-out stage does not exist and a statistical treatment equivalent to the dynamical process has to be adapted to the time window of the experiment [1]. Conversely, the time scales are so short in heavy-ion collisions that well-defined freeze-out time(s) can be identified. However, the underlying dynamical process may very different from the free expansion of a dense system of classical particles. In particular, it is important to stress that macroscopic statistical models in all energy regimes [17,18] suppose that the statistical hypothesis applies at the freeze-out time, and in this sense they by-pass by construction the problem of the out-of-equilibrium evolution up to freeze-out.

In different physical situations flow appears to settle early in the dynamics. Notably, this is the case of central nuclear collisions, where flow is associated with an initial compression of the dinuclear system. In such a situation equilibrium, if ever reached, is approached when the system is still strongly interacting and we may expect the succeeding dynamics to deeply modify the system configurations. In these situations, the model of an initially equilibrated dense molecular system, which is released to expand freely in the vacuum, may bear some pertinent information.

In this paper we compare freeze-out configurations of a freely expanding Lennard-Jones system with different equilibrium models for the same system. We show that, if statistical models are reasonably correct as far as average quantities are concerned, important differences can be seen in the fragmentation patterns. In particular, close to the liquid-gas phase transition unstable configurations, inaccessible to equilibrium models, appear to dominate the dynamics of the expansion.

*Present address: Department of Engineering, University of Leicester, LE1 7RH, UK.

II. ISOBAR MICROCANONICAL ENSEMBLE

The system under study is composed of excited drops made up of $N=147$ particles interacting via a Lennard-Jones (LJ) 6-12 potential $v_{LJ}(r)$ with a cutoff radius $r_c=3\sigma$. Energies are measured in units of the potential well (ϵ), σ characterizes the radius of a particle, and m is its mass. We adopt adimensional units for energy, length, and time such that $\epsilon=\sigma=1$ and $t_0=\sqrt{\sigma^2 m/48\epsilon}$. The initial condition is given by the microcanonical isobar statistical ensemble described by the probability for each microstate (n):

$$p_0^{(n)}=\frac{\delta(E-H_{LJ}^{(n)})}{W_\lambda(E)}\exp\left[-\lambda\sum_{i=1}^{N}(r_i^{(n)})^2\right], \tag{1}$$

where $r_i^{(n)}$ is the position of particle i within the microstate (n), $H_{LJ}^{(n)}$ is the corresponding Lennard-Jones energy, λ is a Lagrange multiplier constraining a finite size, and

$$W_\lambda(E)=\sum_{(n)}\exp\left[-\lambda\sum_{i=1}^{N}(r_i^{(n)})^2\right]\delta(E-H_{LJ}^{(n)}) \tag{2}$$

is the associated density of states or partition sum. The distribution, Eq. (1), is the minimum biased probability distribution for an isolated finite system with a finite size measured by its radius [21]:

$$\langle r^2\rangle=\frac{1}{N}\left\langle\sum_{i=1}^{N}(\vec{r}_i^{(n)})^2\right\rangle_n, \tag{3}$$

where the average is taken over microstates. To generate the statistical ensemble, Eq. (1), we numerically proceed as follows. A harmonic potential with spring constant $k=m\omega^2$, with $\omega=0.1t_0^{-1}$, is added to the Hamiltonian, and the system is coupled to a thermostat using the Andersen technique [19] to achieve equilibrium inside the oscillator. In brief, this is attained by stochastic impulsive forces that act occasionally on randomly selected particles. After each collision, the selected particle is endowed with a new velocity drawn from a Maxwell-Boltzmann distribution at the desired temperature β^{-1}. Between stochastic collisions, the system evolves at constant energy. It has been proved that, under some general conditions [19], the constant energy shells are visited according to their Boltzmann weights, which in turn implies that the ensemble of configurations at different times constitutes a canonical ensemble at the thermostat temperature, distributed as

$$p_{cano}^{(n)}=\frac{1}{Z_{\beta,k}}\exp\left(-\beta\sum_{i=1}^{N}\left[\frac{(\vec{p}_i^{(n)})^2}{2m}+\frac{k}{2}(\vec{r}_i^{(n)})^2\right]+-\beta\sum_{i<j}^{N}v_{LJ}(|\vec{r}_i^{(n)}-\vec{r}_j^{(n)}|)\right). \tag{4}$$

Microcanonical ensembles are extracted at different energies by sorting the events of the canonical distributions according to their energy, excluding the contribution of the confining potential (further details can be found in Refs. [23,24]). These dense configurations correspond for all energies to the supercritical part of the Lennard-Jones phase diagram [20].

III. COMPARISON WITH THE FREELY EXPANDING SYSTEM

A. Choice of comparison time

The equilibrated configurations are let to evolve in the vacuum for a time long enough that the chemical composition of the system is settled (freeze-out time).[1] An interesting observable to study the freeze-out properties of the system is given by the normalized kinetic energy fluctuation $A_K=N\sigma_K^2/\langle K\rangle^2$. This quantity shows a saturation when the sharing between kinetic and potential energy finishes, which physically corresponds to the formation of surfaces within the system, which in turn implies a chemical stabilization of the cluster properties [15]. The behavior of this fluctuation with time is displayed for four representative energy states in the upper part of Fig. 1.

During the time evolution, the initially disordered kinetic energy is partially converted into collective motion, defined as

$$E_{flow}^{(n)}(t)=N\frac{(\vec{p}_r^{(n)})^2}{2m}=\sum_{i=1}^{N}\frac{1}{2m}\left(\vec{p}_i^{(n)}\cdot\frac{\vec{r}_i^{(n)}}{r_i^{(n)}}\right)^2. \tag{5}$$

The internal energy at each time is correspondingly given by $E_{int}=K_{int}+V_{LJ}$, where

$$K_{int}^{(n)}(t)=\sum_{i=1}^{N}\frac{1}{2m}(\vec{p}_i^{(n)}-\vec{p}_r^{(n)})^2, \tag{6}$$

and $V_{LJ}^{(n)}=\Sigma_{i\neq j}v_{LJ}(|\vec{r}_i^{(n)}-\vec{r}_j^{(n)}|)$ is the interaction part of the Lennard-Jones energy.

The time evolution of the system with different initial energies is represented in the $\langle E_{int}\rangle$ versus $\langle r^2\rangle$ plane in the lower part of Fig. 1. We can see that the time evolution corresponds to a rapid expansion and a development of collective flow which enlarges with increasing total energy. If at the entropy-saturation time or freeze-out time t_f the system were still close to statistical equilibrium, it should be described by Eq. (1) with $E=\langle E_{int}\rangle(t_f)$ and a new volume constraint ω such that the average over the statistical ensemble (1) of the mean-square radius is $\langle r^2\rangle=\langle r^2\rangle(t_f)$. The mean-square radius of an equilibrated system with the looser constraint $\omega=0.01t_0^{-1}$ is also represented in the lower part of Fig. 1. The points where this curve intersects the time evolution of the freely expanding systems give the times we have chosen to compare the statistical and dynamical ensembles. As can be seen in the upper part of the figure, these times are long enough for the configurations to be safely considered as frozen for all chosen energies. At later times, the dynamics will not further affect significantly energy and fragment partitions, meaning that the comparison we show will also be pertinent.

[1] For each energy, 1000 events were simulated using the velocity Verlet algorithm. For more technical details on the implementation see Ref. [15].

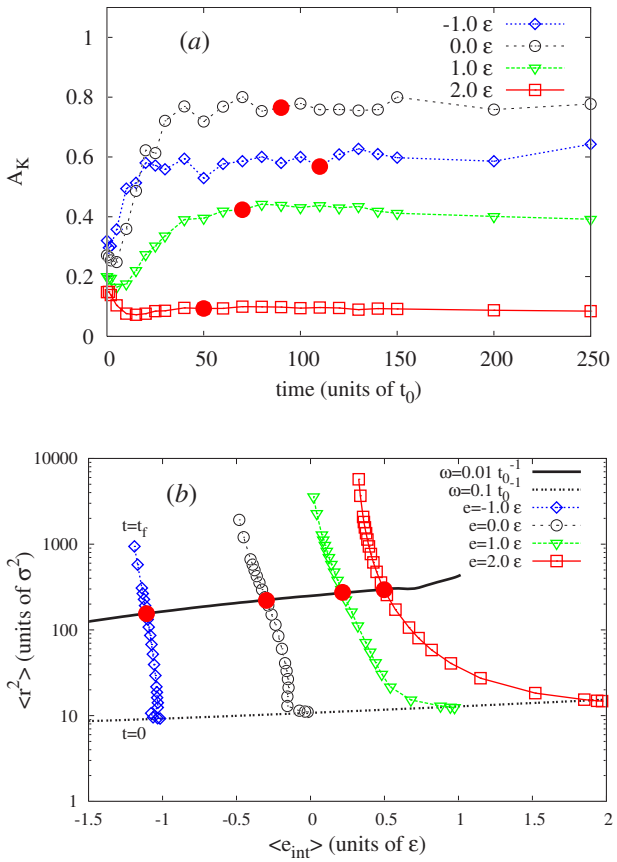

FIG. 1. (Color online) (a) Kinetic energy fluctuation A_K (see text) as a function of time for the freely expanding system at four different energies. (b) Mean-square radius as a function of the internal energy $\langle E_{int}\rangle/N$ of a confined LJ system in a harmonic trap with $\omega=0.01t_0^{-1}$ (solid line) and $\omega=0.1t_0^{-1}$ (dashed line), compared to LJ systems in free expansion, at different total energies and times between $0t_0$ and $t_f=250t_0$ (symbols). The large solid circles in both pictures correspond to the time at which the confined and freely expanding systems have the same mean spatial extension. All quantities are expressed in reduced units.

B. Energy sharing and effective temperature

The time-dependent sharing of the internal energy $E_{int}=K_{int}+V$ between the kinetic and interaction components is shown in Fig. 2, which displays the average disordered kinetic energy $\langle K_{int}\rangle$ as a function of the internal energy for the different evolutions. The equilibrium correlations for the initial and final states are also represented.

We can see that the equilibrium sharing is well verified at the freeze-out time, except for a slight underestimation at the lower energies. This result implies that the kinetic energy at freeze-out, once the collective component is subtracted, can be used as a thermometer measuring a physically well-defined temperature for the expanding system.

The deviation at low energies is also interesting. At $E/N=-1\epsilon$, the system evolution consists essentially of a simple evaporation of monomers and light fragments from the surface of a single excited condensed drop. The poor reproduction by the statistical ansatz (1) of the drop in the kinetic energy implies that the evaporation rate can only approximately be described in terms of an effective pressure [22], due to the irreducible time dependence of the evaporation process.

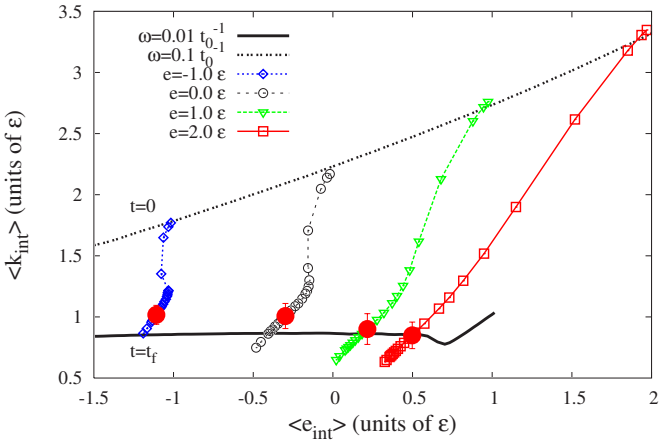

FIG. 2. (Color online) Average kinetic energy per particle, $\langle K_{int}\rangle/N$, as a function of the internal energy per particle, $\langle E_{int}\rangle/N$, of a confined LJ system in a harmonic trap with $\omega=0.01t_0^{-1}$ (solid line) and $\omega=0.1t_0^{-1}$ (dashed line) compared to *LJ* systems in free expansion at different total energies at times between $0t_0$ and $t_f=250t_0$ (symbols). Large solid circles correspond to the time at which the confined and freely expanding systems have the same mean spatial extension. Error bars correspond to one standard deviation, over 1000 events corresponding to each energy.

C. Statistical treatment of the expansion dynamics

At first sight it may be surprising that the best agreement with the equilibrium picture is obtained at the two highest-energy values, where the flow contribution is the most important and the dynamics is the fastest (see Fig. 1). This counterintuitive result can be understood if we consider that the structure (1) for the microstate distribution is exactly preserved by the time evolution in the case of noninteracting particles or local interactions, as we now show [21,23]. For a Hamiltonian system, the time dependence of any mean observation $\langle A\rangle$ is given by $\partial_t\langle A\rangle=-\langle\{H,A\}\rangle$. If the system is noninteracting ($H=K$), this immediately gives

$$\partial_t\langle\vec{r}^2\rangle=\frac{2}{m}\langle\vec{r}\cdot\vec{p}\rangle,$$

$$\partial_t\langle\vec{r}\cdot\vec{p}\rangle=\frac{1}{m}\langle\vec{p}^2\rangle,$$

$$\partial_t\langle\vec{p}^2\rangle=0. \tag{7}$$

It is easy to show that these same relations hold for a non-Hamiltonian dynamics in the presence of a Boltzmann collision integral accounting for local two-body interactions. Let us consider an initial condition given by the equilibrium distribution, Eq. (4) (with $v_{LJ}=0$), imposing given values for the average kinetic energy and mean-square radius through the Lagrange multipliers β and $\lambda=\beta m\omega^2/2$, which constrain the observables $\langle\vec{p}^2\rangle$, and $\langle\vec{r}^2\rangle$, respectively. At any succeeding

time, the exact evolution of these observables will be given by Eqs. (7). The minimum biased distribution, fulfilling the time-dependent constraints and additionally conserving the total energy, is given at any time t by

$$p^{(n)}(t) = \frac{\delta(E - H^{(n)})}{W_\lambda(E,t)} \exp\left[-\tilde{\beta}(t) \sum_{i=1}^{N} \frac{(\vec{p}_i^{(n)})^2}{2m} - \lambda \sum_{i=1}^{N} (\vec{r}_i^{(n)})^2 + \nu(t) \sum_{i=1}^{N} \vec{p}_i^{(n)} \cdot \vec{r}_i^{(n)} \right], \tag{8}$$

with

$$\tilde{\beta}(t) = \frac{2\lambda}{m} t^2, \quad \nu(t) = \frac{2\lambda}{m} t. \tag{9}$$

Using the associated dynamical equation (Liouville equation for the ideal gas or Boltzmann equation for the collision problem), it is possible to show [21] that Eq. (8) is the exact evolution of Eq. (4) under the action of the ideal gas Hamiltonian.

Equation (8) can be interpreted as a self-similar radially expanding ideal gas in local equilibrium with a time-dependent temperature and pressure. Indeed, the distribution can be written as

$$p^{(n)}(t) = \frac{\delta(E - H^{(n)})}{W_\lambda(E,t)} \exp\left[-\tilde{\beta}(t) \sum_{i=1}^{N} \frac{(\vec{p}_i^{(n)} - m\tilde{h}(t)\vec{r}_i^{(n)})^2}{2m} \right], \tag{10}$$

where the collective radial velocity is proportional to the radius (self-similar motion) and $\tilde{h} = 1/t$ represents a Hubble factor.

In the absence of an attractive interparticle interaction, the whole momentum distribution participates in the flow dynamics. As noticed above, in the LJ case a part of the initial kinetic energy is converted into the internal energy of the clusters. Because of the spherical symmetry of the problem $\langle \Sigma_{i=1}^{N} \vec{p}_i \rangle = N \langle \vec{p}_r \rangle$, the two contributions are decoupled, $N\langle \vec{p}^2 \rangle / 2m = \langle K_{int} \rangle + \langle E_{flow} \rangle$ [see Eqs. (5) and (6)] and we can expect Eq. (7) to be still approximately satisfied, provided the internal contribution to the kinetic energy is subtracted. The time evolution of the average square radius, collective flow, and square momentum is represented for different total energies in Fig. 3. At the beginning of the evolution the strong interactions acting in these dense supercritical systems modify the dynamics with respect to the ideal gas or diluted Boltzmann ansatz. However, after $t \approx 20 t_0$, the trend predicted by Eq. (7) is well verified. In a first approximation, the system is still dense and homogeneous at $t \approx 20 t_0$ [15] (see Fig. 1). Therefore, we can make the assumption that at $t \approx 20 t_0 \equiv t_1$ the initial condition (1) still describes the observed distribution with the extra constraint of a collective flow $\langle \vec{p} \cdot \vec{r} \rangle (t_1) \neq 0$:

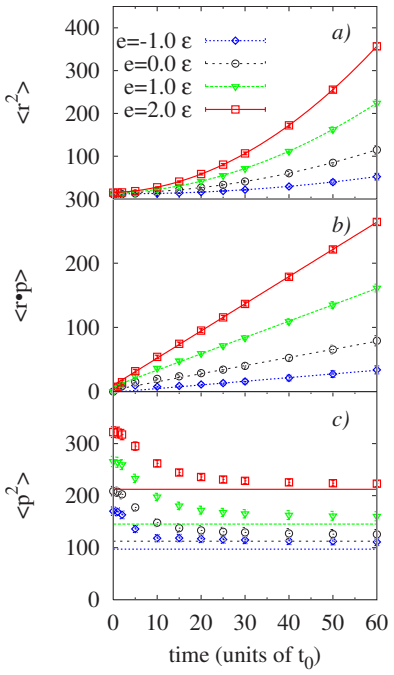

FIG. 3. (Color online) Time dependence of the average square radius (a), radial flow (b), and square momentum (c)—all in reduced units—for the freely expanding system at four different energies. Symbols: numerical simulations, where the internal square momentum of the largest cluster recognized at asymptotic times is subtracted. Lines: free gas evolution Eqs. (15)–(17) corresponding to the statistical ansatz, Eq. (14), with an initial flow.

$$p^{(n)}(t_1) = \frac{\delta(E - H_{LJ}^{(n)})}{W_{\lambda_1}} \exp\left[-\lambda_1 \sum_{i=1}^{N} (\vec{r}_i^{(n)})^2 + \nu_1 \sum_{i=1}^{N} \vec{p}_i^{(n)} \cdot \vec{r}_i^{(n)} \right]. \tag{11}$$

In the ideal or Boltzmann gas limit, the succeeding evolution of the distribution (11) is given again by Eq. (8), with a modification of the time-dependent constraints to account for the initial flow.

As far as average observables are concerned, we can equivalently consider an initial condition in the canonical ensemble, as the different ensembles essentially differ at the level of fluctuations:

$$p_{cano}^{(n)}(t_1) = \frac{1}{Z_{\beta_1,\lambda_1}} \exp\left[-\sum_{i=1}^{N} \beta_1 (\vec{p}_i^{(n)})^2 - \lambda_1 (\vec{r}_i^{(n)})^2 + \nu_1 \sum_{i=1}^{N} \vec{p}_i^{(n)} \cdot \vec{r}_i^{(n)} \right]. \tag{12}$$

This simplification allows a straightforward calculation of the equations of state. Indeed, the time-dependent partition sum can be factorized into $Z_{\tilde{\beta}_1,\tilde{\lambda}_1,\tilde{\nu}_1} = z_{\tilde{\beta}_1,\tilde{\lambda}_1,\tilde{\nu}_1}^{N}$, with

$$z_{\tilde{\beta},\tilde{\lambda},\tilde{\nu}}(t) = \frac{1}{h^3}\int d^3r \int d^3p \left[\exp\left(-\tilde{\beta}_1(t)\frac{\vec{p}^2}{2m} - \tilde{\lambda}_1(t)\vec{r}^2 + \nu_1(t)\vec{p}\cdot\vec{r} \right) \right] = \frac{2\sqrt{\pi m}}{h^3}(2\tilde{\beta}_1\tilde{\lambda}_1 - \tilde{\nu}_1^2 m)^{-3/2}. \tag{13}$$

The time-dependent Lagrange parameters are given by

$$\tilde{\beta}_1(t) = \beta_1 - 2\nu_1\Delta t + \frac{2\lambda_1}{m}\Delta t^2,$$

$$\tilde{\lambda}_1(t) = \lambda_1,$$

$$\tilde{\nu}_1(t) = \nu_1 - \frac{2\lambda_1}{m}\Delta t, \tag{14}$$

and the time-dependent equations of state give, for any $\Delta t = t - t_1 > 0$, the predicted evolution of the average observables:

$$\langle p^2 \rangle = -2m\frac{\partial \ln z_{\tilde{\beta}_1\tilde{\lambda}_1\tilde{\nu}_1}}{\partial \tilde{\beta}_1(t)} = \frac{6m\lambda_1}{2\beta_1\lambda_1 - m\nu_1^2}, \tag{15}$$

$$\langle r^2 \rangle = -\frac{\partial \ln z_{\tilde{\beta}_1\tilde{\lambda}_1\tilde{\nu}_1}}{\partial \tilde{\lambda}_1(t)} = \frac{3\beta_1 - 6\nu_1\Delta t + \frac{6\lambda_1}{m}\Delta t^2}{2\beta_1\lambda_1 - m\nu_1^2}, \tag{16}$$

$$\langle \vec{p}\cdot\vec{r} \rangle = \frac{\partial \ln z_{\tilde{\beta}_1\tilde{\lambda}_1\tilde{\nu}_1}}{\partial \tilde{\nu}_1(t)} = \frac{3m\nu_1 - 6\lambda_1\Delta t}{2\beta_1\lambda_1 - m\nu_1^2}. \tag{17}$$

The good adequacy displayed in Fig. 3 between the numerical evolution and the ideal gas dynamics Eqs. (15)–(17) shows that, as far as average global observables are concerned, the expansion can be represented at any time as a statistical equilibrium in the local rest frame Eq. (8), even in the diabatic limit. It also confirms the expected equivalence between the microcanonical and canonical average evolution.

D. Deviations from equilibrium

The good reproduction of the time-dependent average observables by the equilibrium ansatz does not mean that the configurations explored by the expanding system coincide with the equilibrium configurations. To look for deviations from equilibrium, we first show in Fig. 4 the behavior of potential energy fluctuations. In the low-energy liquid regime, as well as near the liquid-gas transition, the freeze-out fluctuations for the freely expanding system are very close to the prediction of the equilibrium model without flow. However, for intermediate energies ($E/N=0\epsilon, E/N=1\epsilon$), the fluctuations are underestimated by the equilibrium calculation.

This underestimation can be partly due to the energy conservation constraint. Indeed, in the expansion of an isolated system the total energy is a constant of motion. This means that the potential energy can be converted both into internal kinetic energy and into collective flow, inducing event-by-event fluctuations in both components. This effect is not considered in Eq. (1) where the flow is absent, and the conservation law therefore applies to the total internal energy. In other words, the equilibrium ansatz (1) disregards flow energy fluctuations.

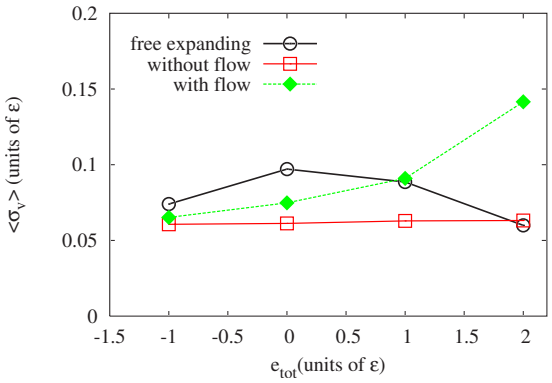

FIG. 4. (Color online) Potential energy per particle fluctuations for the freely expanding (open circles), constrained without flow [Eq. (1)] (open squares) and constrained with flow [Eq. (11)] (solid diamonds) systems. The abscissa gives the total energy per particle, E_{tot}/N, of the freely expanding system in all cases.

To quantify this effect and assess if the fluctuation underestimation can be explained by it, we have also plotted in Fig. 4 the prediction of Eq. (11).

To numerically simulate Eq. (11) we first consider its canonical counterpart Eq. (12) which can again be recast as an isobar equilibrium in the expanding frame

$$p^{(n)}(t) = \frac{1}{Z_{\beta_1,\lambda_1'}}\exp\left[-\sum_{i=1}^{N}\beta_1(t)\frac{[\vec{p}_i^{(n)} - mh_1(t)\vec{r}_i^{(n)}]^2}{2m} + \lambda_1'(\vec{r}_i^{(n)})^2 \right], \tag{18}$$

with $h_1=\nu_1/\beta_1$ and $\lambda_1'=\lambda_1-m\nu_1^2/2\beta_1$. This distribution is simulated as Eq. (4) above. Then a radial momentum $\vec{p}_r = mh_1\vec{r}$ is added to each particle and a microcanonical sorting is imposed on the total energy including flow, $E' = \Sigma_i(\vec{p}_i + \vec{p}_{ri})^2/(2m) + V_{LJ}$ [23].

Thus, three models are compared in this figure: the freely expanding system at time t_f and the equilibrium model in the local rest frame including [Eq. (11)] and not including [Eq. (1)] flow fluctuations. The three models are tuned to have, on average, the same internal energy $\langle E_{int} \rangle$ and spatial extension $\langle r^2 \rangle$. This internal energy is fixed in each event (n), $K^{(n)} + V^{(n)} = E_{int} = \text{const}$, in the case of Eq. (1); while it can fluctuate in the free expansion and also for Eq. (11), where $K^{(n)} + V^{(n)} = E_{int}^{(n)} + E_{flow}^{(n)} = E_{tot} = \text{const}$. We can see from Fig. 4 that flow fluctuations can enhance the potential energy variance, but they cannot explain the deviation as they do not exhibit the correct energy dependence. Indeed, at the highest energy considered, Eq. (11) strongly overshoots the expanding simulation.

To understand the origin of this deviation, we plot in Fig. 5 the matter density and radial velocity profiles associated

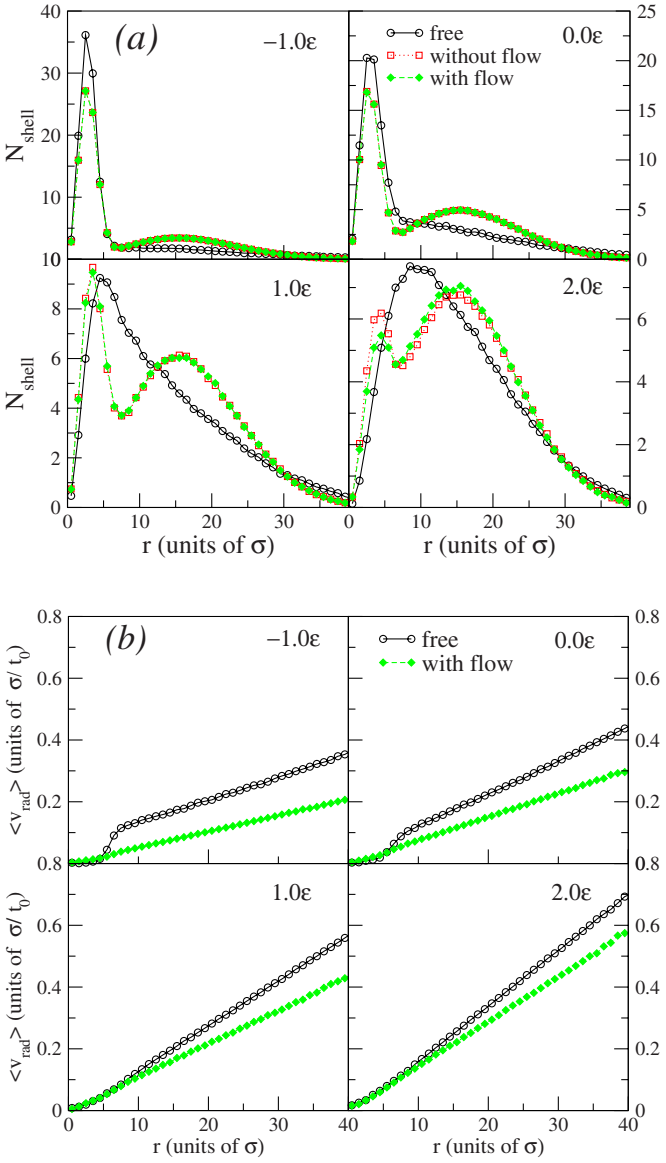

FIG. 5. (Color online) (a) Average number of particles located in a spherical shell of radius r as a function of r, calculated from the center of mass of the system. (b) Average velocity in the radial direction in the same spherical shells used in (a). The four energies (-1.0ϵ, 0.0ϵ, 1.0ϵ, and 2.0ϵ) and the three models [free expansion (open circles), equilibrium in the local rest frame with (solid diamonds), and without (open squares) flow fluctuations] are displayed.

with the four different energies and the three models previously shown in Fig. 4. The statistical simulations always present a well-pronounced density peak close to the center of mass of the system, corresponding to a single drop of decreasing size. The rest of the matter concentrates on a second density peak around $r \approx 15\sigma$, where most of the clusters are located.

The spatial distribution of matter for the freely expanding system is close to this picture at the lowest energy under analysis. However, the presence of a heavy drop close to the center of mass modifies the shape of the radial flow, which is very far away from the self-similar assumption of Eq. (11).

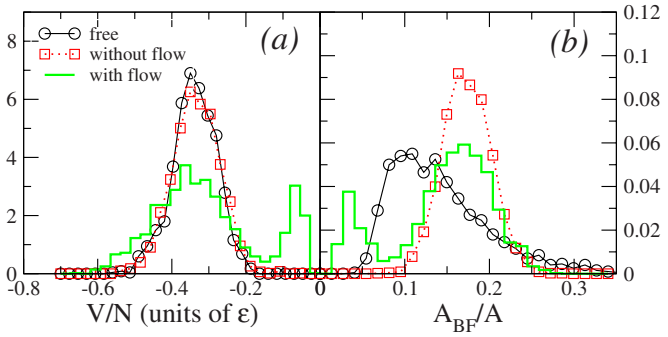

FIG. 6. (Color online) Distributions of potential energy (a) and of the size of the largest MST fragment (b) for the highest energy considered (2.0ϵ) and the three models (free expansion and equilibrium in the local rest frame with and without flow fluctuations).

The Hubble flow in Eq. (11) comes from the ideal-gas equations of motion [Eq. (7)]. We can see from Fig. 5 that the interparticle LJ interaction cannot be neglected in the dense part of the system, which leads to an important deviation from self-similarity. We expect that a better description of the expansion dynamics would be obtained by considering for the flow dynamics in Eq. (11) clusters instead of single-particle degrees of freedom, as in the standard Fisher picture of condensation [25]. At higher energies, the two distributions are completely different. Indeed, the central drop progressively disappears, leading to a smoother matter distribution along the radial direction. From previous studies [16], we know that the resulting large bump corresponds to a high multiplicity of clusters of approximately equal size. The presence of clusterized matter leads to a deviation from the Hubble flow even at the highest energy considered.

More information on the specific configurations accessed by the flow dynamics can be obtained from Fig. 6. This figure displays the distributions of the potential energy and of the size of the largest fragment recognized through the MST algorithm [16]. It confirms that the freely expanding system explores configurations which are very different from the equilibrium case. As already observed in Fig. 2, the global energy sharing between the potential and kinetic energy of the freely expanding system is consistent with equilibrium, and consequently the potential energy distributions are close. However, the associated partitions are very different and tend to be more fragmented in the freely expanding case, as shown by the fact that the largest cluster size distribution is broader and peaked at a lower value. At the particular energy shown in the figure, the system is close to the liquid-gas phase transition. If flow fluctuations are allowed, as in Eq. (11), some gas partitions can be explored, leading to the bimodal distributions observed in Fig. 6. Interestingly, the fact that a statistical treatment of flow can lead to bimodality was recently observed in Ref. [23]. The presence of bimodal distributions explains the severe overestimation of the freely expanding system fluctuations shown in Fig. 4. Indeed, a potential energy barrier has to be overcome to access these distributions during the actual time evolution of the expansion and this does not seem to occur easily for the freely expanding system. As was already shown in Ref. [26], flow acts as a heat sink, precluding the exploration of gas configu-

rations. The largest cluster distribution shows that most partitions of the freely expanding system present an intermediate degree of fragmentation between liquid and gas. Such partitions are metastable or unstable at equilibrium, but can be accessed in the free expansion due to the short time scale of the dynamics.

IV. CONCLUSIONS

In this paper we have compared the diabatic expansion dynamics of a Lennard-Jones system, initially confined in a harmonic oscillator and subsequently expanding freely in the vacuum, with a statistical ansatz in the hypothesis of a purely Hubble flow. This hypothesis is exact in the limiting case of a noninteracting system or a Boltzmann dynamics. For our strongly interacting system, the presence of finite range two-body interactions is known [21] to modify the Hubble approximation, introducing non-self-similar flow components. In a future work, it will be very interesting to explore the adequacy of a more sophisticated statistical ansatz including non-self-similar flows, to reproduce the dynamics of the expansion. In the present paper, a self-similar approximation has been revealed to be accurate enough to reasonably describe the mean value of global one-body observables at all times. As soon as more sophisticated observables are examined, discrepancies arise. In the self-similar statistical ansatz, flow does not modify the partitions in configuration space, but it acts as a heat bath, allowing important energy fluctuations and the exploration of the unbound gas phase. In the diabatic dynamics, such configurations are never reached and metastable highly clusterized partitions dominate. Interestingly, qualitatively similar behaviors have recently been observed in an analysis of nuclear multifragmentation data [27] by means of a detailed comparison between the fragmentation of central and peripheral collisions.

ACKNOWLEDGMENTS

Partial support from the University of Buenos Aires via Grant No. X360 is acknowledged. M.J.I. also acknowledges the kind hospitality of the LPC, where the core of the work was developed, as well as financial support from the LPC, the University of Buenos Aires, and Fundacion Antorchas. F.G. acknowledges partial support from the Institut Universitaire de France. C.O.D. acknowledges partial support from CONICET.

[1] C. Bréchignac, Ph. Cahuzac, B. Concina, and J. Leygnier, Phys. Rev. Lett. **89**, 203401 (2002).
[2] M. Schmidt, T. Hippler, J. Donges, W. Kronmuller, B. von Issendorff, H. Haberland, and P. Labastie, Phys. Rev. Lett. **87**, 203402 (2001).
[3] P. Brockhaus, K. Wong, K. Hansen, V. Kasperovich, G. Tikhonov, and V. V. Kresin, Phys. Rev. A **59**, 495 (1999).
[4] G. Martinet *et al.*, Phys. Rev. Lett. **93**, 063401 (2004).
[5] F. Gobet, B. Farizon, M. Farizon, M. J. Gaillard, J. P. Buchet, M. Carre, P. Scheier, and T. D. Mark, Phys. Rev. Lett. **89**, 183403 (2002).
[6] K. Gluch, S. Matt-Leubner, O. Echt, B. Concina, P. Scheier, and T. D. J. Mark, Chem. Phys. **121**, 2137 (2004).
[7] C. E. Klots, Nature (London) **327**, 222 (1987).
[8] F. Calvo, J. Phys. Chem. A **110**, 1561 (2006).
[9] *Dynamics and Thermodynamics with Nuclear Degrees of Freedom*, edited by Ph. Chomaz, F. Gulminelli, W. Trautmann, and S. Yennello (Springer, Berlin, 2006).
[10] W. Reisdorf *et al.*, Phys. Lett. B **595**, 118 (2004).
[11] E. V. Shuryak, e-print arXiv:hep-ph/0608177.
[12] L. W. Chen and C. M. Ko, Phys. Lett. B **634**, 205 (2006).
[13] V. N. Russkikh and Yu. B. Ivanov, Phys. Rev. C **74**, 034904 (2006).
[14] X. Campi, H. Krivine, E. Plagnol, and N. Sator, Phys. Rev. C **67**, 044610 (2003).
[15] A. Chernomoretz, F. Gulminelli, M. J. Ison, and C. O. Dorso, Phys. Rev. C **69**, 034610 (2004).
[16] A. Strachan and C. O. Dorso, Phys. Rev. C **58**, R632 (1998); **59**, 285 (1999).
[17] J. P. Bondorf, A. S. Botvina, A. S. Iljinov, I. N. Mishustin, and K. Sneppen, Phys. Rep. **257**, 133 (1995).
[18] F. Becattini, J. Manninen, and M. Gazdzicki, Phys. Rev. C **73**, 044905 (2006); A. Andronic, P. Braun-Munzinger, and J. Stachel, Nucl. Phys. A. **772**, 167 (2006).
[19] H. C. Andersen, J. Chem. Phys. **72**, 2384 (1980).
[20] A. Chernomoretz, P. Balenzuela, and C. Dorso, Nucl. Phys. A. **723**, 229 (2003).
[21] Ph. Chomaz, F. Gulminelli, and O. Juillet, Ann. Phys. (N.Y.) **320**, 135 (2005).
[22] L. G. Moretto, J. B. Elliott, and L. Phair, Phys. Rev. C **72**, 064605 (2005).
[23] M. J. Ison, F. Gulminelli, and C. O. Dorso, Phys. Rev. E **76**, 051120 (2007).
[24] F. Gulminelli, Ph. Chomaz, and V. Duflot, Europhys. Lett. **50**, 434 (2000).
[25] M. E. Fisher, Physics (Long Island City, N.Y.) **3**, 255 (1967).
[26] A. Chernomoretz, M. Ison, S. Ortiz, and C. O. Dorso, Phys. Rev. C **64**, 024606 (2001).
[27] E. Bonnet, Ph.D. thesis, Universite de Paris-Sud XI, Orsay, 2006 (unpublished); N. Le Neindre *et al.*, Nucl. Phys. A. **795**, 47 (2007).